Polar Biology (2023) 46:339–355
https://doi.org/10.1007/s00300-023-03127-7

ORIGINAL PAPER

First report on biological iron uptake in the Antarctic sea-ice environment

Delphine Lannuzel[1,2] · Marion Fourquez[3] · Jeroen de Jong[4] · Jean-Louis Tison[5] · Bruno Delille[6] · Véronique Schoemann[4,7]

Received: 15 May 2022 / Revised: 3 March 2023 / Accepted: 23 March 2023 / Published online: 7 April 2023

Abstract

Melting sea ice is a seasonal source of iron (Fe) to the Southern Ocean (SO), where Fe levels in surface waters are otherwise generally too low to support phytoplankton growth. However, the effectiveness of sea-ice Fe fertilization in stimulating SO primary production is unknown since no data exist on Fe uptake by microorganisms in the sea-ice environment. This study reports a unique dataset on Fe uptake rates, Fe-to-carbon (C) uptake ratio (Fe uptake normalized to C uptake) and Fe:C uptake rate (Fe uptake normalized to biomass) by in situ microbial communities inhabiting sea ice and the underlying seawater. Radioisotopes ^{55}Fe and ^{14}C were used in short-term uptake experiments during the 32-day Ice Station POLarstern (ISPOL) time series to evaluate the contributions of small (0.8–10 µm) and large (> 10 µm) microbes to Fe uptake. Overall, results show that over 90% of Fe was bound to the outside of the cells. Intracellular Fe (Fe_{intra}) uptake rates reached up to 68, 194, and 203 pmol Fe $L^{-1}d^{-1}$ in under-ice seawater, bottom ice, and top ice, respectively. Inorganic carbon uptake ranged between 0.03 and 3.2 µmol C L^{-1} d^{-1}, with the lowest rate observed in under-ice seawater. Importantly, between the start and end of ISPOL, we observed a 30-fold increase in Fe_{intra} normalized to carbon biomass in bottom sea ice. This trend was likely due to changes in the microbial community from a dominance of large diatoms at the start of the survey to small diatoms later in the season. As the Antarctic icescape and associated ecosystems are changing, this dataset will help inform the parameterisation of sea-ice biogeochemical and ecological models in ice-covered regions.

Keywords Sea ice · Fe:C ratio · Ice algae · Phytoplankton · Uptake rates

✉ Delphine Lannuzel
delphine.lannuzel@utas.edu.au

1 Institute for Marine and Antarctic Studies, University of Tasmania, 20 Castray Esplanade, Hobart, TAS 7001, Australia

2 Australian Centre for Excellence in Antarctic Science, University of Tasmania, 20 Castray Esplanade, Hobart, TAS 7001, Australia

3 Aix Marseille Univ, Université de Toulon, CNRS, IRD, MIO UMR 110, 13288 Marseille, France

4 Laboratoire G-Time, Université Libre de Bruxelles, Brussels, Belgium

5 PROPICE Unit, Laboratoire de Glaciologie, Université Libre de Bruxelles, Brussels, Belgium

6 Unité d'Océanographie Chimique, Freshwater and Oceanic sCience Unit reSearch (FOCUS), Université de Liège, Liège, Belgium

7 Ecology of Aquatic Systems, Faculty of Sciences, Université Libre de Bruxelles, Brussels, Belgium

Introduction

About 30% of the ocean primary productivity in our global ocean is limited by low levels of iron (Fe) in surface waters (Moore et al. 2013). The Southern Ocean (SO) is a prime example where high concentrations of macro-nutrients (nitrate, phosphate, and silicic acid) do not translate into high phytoplankton biomass because of this Fe limitation. However, some naturally Fe-fertilized biological hotspots do exist in the SO, such as downstream of island plateaus (Blain et al. 2007; Planquette et al. 2007, 2011; Pollard et al. 2009), coastal polynyas (Arrigo and van Dijken 2003; St-Laurent et al. 2019; Moreau et al. 2019), or in the vicinity of floating icebergs (Raiswell et al. 2008; Lin et al. 2011; Shaw et al. 2011; Duprat et al. 2016; Hopwood 2018) and melting glaciers (Raiswell et al. 2006; Gerringa et al. 2012; Herraiz-Borreguero et al. 2016; van der Merwe et al. 2019). The sea-ice zone has been identified as another biologically productive area, where sea ice acts as a seasonal Fe reservoir (Sedwick and DiTullio 1997;

Lancelot et al. 2009; Lannuzel et al. 2016). During winter, when sea ice forms, it concentrates Fe and organic matter from seawater (Gradinger and Ikavalko 1998; Janssens et al. 2016; Person et al. 2020). When sea ice melts in spring, it releases Fe and organic matter in the surface layer of the ocean, therefore stimulating phytoplankton growth in surrounding waters and beyond (Smith and Nelson 1985; Lannuzel et al. 2013; Lieser et al. 2015). This seasonal and widespread fertilization represents the largest source of Fe in the seasonal ice zone in spring (Lannuzel et al. 2007; de Jong et al. 2015), an area that covers approximately 40% of the SO.

Whilst quantifying the magnitude of the Fe supply in seasonally ice-covered waters is paramount, we need data on Fe uptake rates by the microbial community as a mean to estimate biological Fe demand. Some information is available for open ocean phytoplankton (Strzepek et al. 2005; Frew et al. 2006; Sarthou et al. 2008), but no studies have attempted to quantify Fe uptake by sea-ice (sympagic) algae and under-ice (cryopelagic) phytoplankton. Therefore, modellers have had to use alternative ways to parameterize Fe and C dynamics in sea-ice biogeochemical models (Lancelot et al. 2009; Wang et al. 2014; Jeffery et al. 2020). For instance, measurements of dissolved Fe (DFe) concentrations in sea ice were used together with constant intracellular Fe to C molar ratio for phytoplankton (Fe_{intra}:C, see Table 1 for a description of abbreviations) to estimate the Fe-fuelled primary productivity during melting (de Jong et al. 2013; 2015). However, these Fe_{intra}:C ratios are generally based on laboratory culture experiments (Brand 1991; Twining et al. 2004; Sarthou et al. 2005; Hassler and Schoemann 2009; Strzepek et al. 2011; Twining and Baines 2013) that are not representative of the sea-ice environment.

The ranges of Fe_{intra}:C ratios for SO phytoplankton reported in the literature are also large, fuelling more uncertainty. At steady state, the Fe_{intra}:C ratio for phytoplanktonic cells vary between ~ 5 and 50 µmol Fe mol^{-1} C but can reach > 100 µmol Fe mol^{-1} C in the case of artificial Fe enrichments (Boyd et al. 2000; Fourquez et al. 2020). Total (extracellular + intracellular) and intracellular Fe and C contents also vary by several orders of magnitude depending on the type and size of phytoplankton (Veldhuis et al. 2005; Sarthou et al. 2005), the ambient DFe concentrations (Sunda and Huntsman 1995; Maldonado and Price 1996; Bruland et al. 2001; Sarthou et al. 2005), and/or in situ nutrient gradients (Twining et al. 2021). Therefore, overestimating algal Fe uptake may result in an underestimation of primary production and C export (and vice versa). Measurements of Fe:C ratios in and under sea ice are therefore crucially needed to properly constrain the efficiency of the biological pump of carbon in this climate-sensitive environment.

Since large physical and chemical gradients are encountered in sea ice, algal cell concentrations can vary by up to six orders of magnitude (from $< 10^4$ to 10^9 cells L^{-1}). Low values in the upper ice cover are typical of oceanic waters, whilst some of the highest values for any aquatic environment can be recorded at the sea ice/seawater interface (Lizotte 2003). Consequently, for this study we chose to target several sea-ice horizons to get a holistic view of how environmental conditions may affect Fe uptake rates both within and under sea ice. We carried out short-term (4–6 h) incubation experiments to measure Fe and inorganic carbon uptake by microbial communities inhabiting slush (a naturally occurring mixture of snow and seawater), bottom sea ice as well as seawater (right below sea ice). The use of radiotracers (^{55}Fe and ^{14}C) and a chemical wash allowed an estimation of the rates of incorporation into biomass (intracellular) but also around the cells (extracellular). Measuring Fe_{intra} is of prime interest to quantify cellular Fe needed to sustain biological activities, whilst measuring extracellular Fe ($Fe_{extra} = Fe_{tot} — Fe_{intra}$) is paramount for the construction of biogeochemical Fe budgets. Our study focuses on the behaviour of sea-ice algae and phytoplankton but we also discussed the role of other organisms (bacteria and protists) naturally present in our incubations.

Materials and methods

Sampling and analytical methods for the main variables

Sea ice, brine, seawater, and slush were collected in the Antarctic pack ice zone during the Ice Station POLarstern (ISPOL) research cruise onboard the RV *Polarstern* from 29th November to 31st December 2004 in the Western Weddell Sea (68°S 55°W). In situ sea-ice temperatures were measured using a calibrated probe (TESTO 720) inserted every 5 cm along a freshly sampled core. Precision of the

Table 1 List of abbreviations

Symbol	Meaning	Unit
Fe_{tot}	Total (intracellular+extracellular) ^{55}Fe uptake rate	pmol L^{-1} d^{-1}
Fe_{intra}	Intracellular ^{55}Fe uptake rate	pmol L^{-1} d^{-1}
Fe_{intra}:C	Intracellular ^{55}Fe uptake rate normalized to inorganic ^{14}C uptake rate	µmol Fe mol^{-1} C
Fe_{intra}:POC	Intracellular ^{55}Fe uptake rate normalized to particulate organic carbon	µmol Fe mol^{-1} C d^{-1}
Fe_{tot}:C	Total ^{55}Fe uptake rate normalized to inorganic ^{14}C uptake rate	µmol Fe mol^{-1} C
Fe_{tot}:POC	Total ^{55}Fe uptake rate normalized to particulate organic carbon	µmol Fe mol^{-1} C d^{-1}

measurements was ± 0.1 °C (Tison et al. 2008). Ice-core sections were melted in the dark at 4 °C in 0.2-µm-pre-filtered seawater (1:4 volume ratio). Chlorophyll a (Chl a) was quantified by fluorometry following filtration of 1 L to 2 L (depending on particle load in the sample) onto 0.7-µm Whatman glass-fibre filters (GF/F) after 90% v:v acetone extraction of the particulate material retained on the filter, in the dark for 12 h at 4 °C (Yentsch and Menzel 1963). Algae and protozoa were enumerated by inverted light microscopy (Utermöhl 1958) and epifluorescence microscopy after DAPI staining (Porter and Feig 1980). Algae and protozoa biomasses were estimated from cell biovolumes using a set of geometric correspondences (Hillebrand et al. 1999) and specific carbon to volume relationship (Menden-Deuer and Lessard 2000). Meltwater for particulate organic carbon (POC) was collected on pre-combusted (450 °C, 4 h) GF/F filters and stored in polystyrene Petri dishes at − 20 °C until analysis in the home laboratory using a FisonsNA-1500 elemental analyser (Dumont et al. 2009). Dissolved Fe (operational fraction < 0.2 µm) was analysed directly onboard by Flow Injection Analysis (FIA) 24 h after acidification with ultrapure HCl (Seastar Baseline) to pH 1.8. The FIA method was adapted from automated continuous flow system (FeLume, Waterville Analytical, USA) that detects chemiluminescence from the reaction of luminol and Fe (II). The detection limit (3σ of the blank) was on average 0.12 nM and the analysis of referenced materials NASS-5 and CASS-3 agreed well with the certified values (Lannuzel et al. 2008).

Sampling strategy for the uptake experiments

Cleaning procedures

All labware used for sampling and incubation was cleaned following strict trace metal clean procedures. Polycarbonate (PC) petri dishes (0.14 m internal diameter, 15 mm thickness), 20-L PC carboys, and 400-mL and 250-mL PC bottles (all Nalgene®) used for Fe incubations were soaked in a detergent bath (RBS 5% v:v) for 24 h, followed by 3 rinses with deionized water and 3 rinses with Ultra High-Purity (UHP) water (18.2 MΩ, Millipore Milli-Q system) before being filled with 1-M HCl (Merck, reagent grade) for 1 week. Each item was rinsed 5 times with UHP water and dried inside a class 100 laminar flow hood. High-density polyethylene (HDPE) melting containers and 250-mL low-density polyethylene (LDPE) bottles were treated the same way, albeit with a stronger acid soak (6-M HCl, Merck, reagent grade). Acid-cleaned bottles and containers were sealed in triple plastic bags until use.

Sampling of seawater, brine, slush, and sea ice

Samples for the uptake experiments were collected on four occasions for sea ice and on one occasion for slush and seawater (Table 2). Core were collected with a 14-cm diameter corer using the trace metal clean techniques described in Lannuzel et al. (2006). As sea ice is a very heterogeneous environment, the cores were collected only 20 cm apart to reduce the uncertainty linked to spatial variability. The cores were transported to the ship, placed in a polyethylene (PE) lathe under class 100 laminar flow, and 1 cm thick of bottom slice were carefully cut along the cores using titanium chisels and blades (Fig. 1). The ice sections were then transferred into acid-washed PC dishes of 14 cm diameter. Surface-ice slush and under-ice seawater sample were also collected on one occasion. The slush sample was collected on Day 22 at the snow/ice interface, using an acid-clean PE shovel, and transferred into trace metal clean 250-mL PC bottles. The seawater sample was sampled on Day 23 at the ice/water interface, using an acid-cleaned braided PVC flexible tube and portable peristaltic pump (Cole-Parmer, Masterflex E/P) with acid-cleaned C-flex pump tubing and collected into acid-clean 250- and 400-mL PC bottles.

Additional seawater and brine were collected to preserve the integrity and environmental conditions of the experiments. Briefly, large volumes of seawater were collected from 30 m below sea ice using an acid-cleaned braided PVC flexible tube and a portable peristaltic pump (Cole-Parmer, Masterflex E/P) with acid-cleaned C-flex pump tubing connected to an acid-cleaned 0.2 µm cartridge filter (Sartorius Sartroban® 300) and transferred into 20-L acid-clean PC carboys. The carboys were stored onboard the ship in the

Table 2 Summary information on the short-term ^{55}Fe and ^{14}C uptake experiments

Sample type	Date	Day of time series	Incubation type	Incubation temperature(°C)	In situ DFe (nmol L^{-1})[a]	^{55}Fe added (nmol L^{-1})
Slush	21-Dec	22	Shipboard	− 1.0	2.54	0.03
Seawater	22-Dec	23	Shipboard	− 1.0	1.52	0.05
Bottom sea ice	5-Dec	6	Shipboard	− 1.9	19.6	0.66
Bottom sea ice	20-Dec	21	In situ	− 1.8	3.00	0.78
Bottom sea ice	28-Dec	29	Shipboard	− 1.6	2.90	1.4
Bottom sea ice	31-Dec	32	In situ	− 1.4	2.90	0.9

[a]Estimated from comparable samples after accounting for background DFe in the spike solutions

Fig. 1 Photographs of (left) ice-core cutting process and (right) sample placement for the in situ incubation. 1-cm-thick slices of sea-ice cores were cut using titanium chisels and blades under a class 100 laminar flow hood; bottom ice slices were transferred into acid-washed polycarbonate dishes of 14 cm diameter and spiked with ^{14}C or ^{55}Fe. Reconstructed cores were inserted into the original core hole in the sea-ice cover, marking the start of the in situ experiment

dark at 4 °C until needed. This filtered seawater was used for two procedural purposes: 1) to melt the incubated sea-ice sections at a 4:1 (v:v) ratio to avoid thermal shock and cell damage and 2) as a spike solution for the slush incubation. Sea-ice brines were also needed for the preparation of the radiotracer solution for the bottom sea-ice incubations. For this purpose, sea-ice brines were drained in situ at 0.6 m deep in the ice cover using the sack-hole technique and collected using the same equipment as for seawater (Tison et al. 2008). The 0.2-µm-filtered brines were collected into an acid-clean 250-mL LDPE bottles previously rinsed with the collected brines. The brines were stored onboard the ship in the dark at 4 °C until needed.

Methods for ^{55}Fe and ^{14}C uptake experiments

Sea ice

The emission spectrum of ^{55}Fe and ^{14}C partly overlap, therefore two separate sea-ice cores were collected at the same time and 20 cm apart to allow better interpretation of the ^{55}Fe and ^{14}C results. For Fe uptake rate measurement, a 1-cm-thick bottom sea-ice slice was spiked with 3 mL of pre-filtered brine (< 0.2 µm) mixed with 17 µL of ^{55}Fe (as $^{55}FeCl_3$, 266 µCi mL^{-1} specific activity Perkin Elmer). The final ^{55}Fe concentrations in the sea-ice samples ranged from 0.7 to 1.4 nmol L^{-1}, depending on the sea-ice brine volume fraction. For inorganic C uptake rate measurement, a second 1-cm-thick slice from a nearby core was spiked with 3 mL of pre-filtered brine (< 0.2 µm) mixed with 20 µL of ^{14}C source solution (as $NaH^{14}CO_3$, 1 mCi mL^{-1}, specific activity 50–60 mCi mmol^{-1}, Amersham Biosciences). The Petri dishes containing the slices were immediately sealed in a transparent plastic zip-lock bag and re-inserted at their original depth together with the remaining ice core sections. The reconstructed ice cores were then transferred into a triple-layered transparent plastic bag and returned to the original core hole (Fig. 1). The core holes were covered with snow to the original snow thickness (11 cm on Day 21 and 6 cm Day 32). This moment marked the start of the in situ incubation period. In situ sea-ice incubations were performed for 5–6 h during ISPOL on two separate occasions (Day 21 and Day 32). Short-term incubations of 5–6 h were also performed shipboard with 1-cm-thick slices of bottom sea ice in the ship's culture room under set temperature (− 1 ± 1 °C) and light (50 µmol m^{-2} s^{-1}) conditions on two separate occasions (Day 6 and Day 29) to mimic the general in situ conditions.

Slush and under-ice seawater

The 250-mL PC bottles filled with slush were spiked with 3 mL of pre-filtered seawater (< 0.2 µm) with 1.5 µL of the $^{55}FeCl_3$ source solution. The final ^{55}Fe concentration in the amended slush was about 0.03 nmol L^{-1} of ^{55}Fe. Another 250-mL PC bottle filled with slush was spiked with 3 mL of pre-filtered seawater (< 0.2 µm) with 25 µL of ^{14}C source solution.

For the seawater incubation, 2.5 µL of ^{55}Fe source was added directly to a 400-mL PC bottles containing the seawater sample (final ^{55}Fe concentration 0.05 nmol L^{-1}). Another 250-mL PC bottle filled with seawater was spiked directly with 25 µL of ^{14}C source solution. The PC bottles were sealed in a zip-lock bag and incubated for 5–6 h in the shipboard culture room.

Filtration procedures

At the end of the incubation period, the ice cores were removed from the ice floe, immediately covered with black plastic bags, and transported to the laboratory of the *RV*

Polarstern. The sea-ice sections were left to melt in 0.2-µm filtered seawater, in the dark and at ambient temperature of the laboratory (melting time 1 h). The samples were subsequently filtered when temperature was still close to 0 °C according to Rintala et al. (2014).

The samples spiked with ^{55}Fe were split in two and then sequentially filtered onto 0.8-µm and 10-µm PC membranes (Nuclepore) to distinguish the amounts of ^{55}Fe incorporated by large (> 10 µm) from small (0.8–10 µm) microorganisms. For each size fraction, total and intracellular ^{55}Fe were counted on separate filters. For total ^{55}Fe measurements, cells collected on the filters were only rinsed once with 5 mL of 0.2-µm filtered seawater. For ^{55}Fe intracellular measurements, cells collected on the filters were rinsed with a freshly prepared Ti-citrate-EDTA wash solution (Tang and Morel 2006) to eliminate non-incorporated ^{55}Fe (extracellular and abiotic adsorption on filter). The wash solution was applied directly on the filters for 2 min, followed by a rinse for 2 min with 5 mL of 0.2-µm filtered seawater (Hudson and Morel 1989; Hassler and Schoemann 2009b).

The samples spiked with ^{14}C were entirely filtered onto 25 mm GF/F membranes (0.7 µm pore size, Whatman). The filters were first rinsed with filtered seawater to reduce the background ^{14}C in the DIC in the dissolved inorganic carbon (DIC) pool and allowed to dry in a desiccator for 1 h under a fume hood before 200 µl of HCl 0.1 N was added onto each filter to allow the DIC to evaporate overnight. Therefore, only organic ^{14}C integrated in biomass remained on the filter. Note that the GF/F filters used for the filtrations from the ^{14}C incubations tend to retain more organic carbon (and associated Fe) than the PC filters used for the ^{55}Fe incubations (Morán et al. 1999).

Finally, all filters were transferred into separate scintillation vials and 10 mL of scintillation cocktail (Ready Safe™, Perkin Elmer) were added. After vortex agitation, the radioactivity on filter (^{55}Fe or ^{14}C) was counted by liquid scintillation counter (Packard). Counts per minute (cpm) were then converted into disintegration per minute using ^{55}Fe and ^{14}C custom quench curves.

Molar uptake rates of Fe (mol Fe L^{-1} d^{-1}) were then calculated as follows:

$$\frac{A \times {}^{55}\,Fe\,on\,filter}{t \times V}.$$

with

$$A = \frac{mol^{55}Fe\,added + mol\,D\,Fe\,in\,situ}{mol^{55}Fe\,added},$$

where V = volume filtered (corrected for dilution), t = incubation time, and cpm = counts per minute

In situ DFe concentrations in the samples (Table 2) were estimated from the DFe concentration measured by Lannuzel et al. (2008) and corrected for the background DFe concentration in the 3-mL spike solution (brine DFe = 9.6 nmol L^{-1} and 30-m seawater = 1.2 nmol L^{-1}).

The Fe_{tot} uptake rates of the cells rinsed with filtered seawater represent whole-cell Fe contents, whilst the ratios of Ti-rinsed cells provide an indication of internal Fe contents (Fe_{intra}). Fe_{intra} by small microorganisms (0.8–10 µm) was estimated by calculating the difference between Fe_{intra} of the whole community (> 0.8 µm) and the Fe_{intra} by large organisms (> 10 µm). Extracellular Fe uptake rates were calculated as the difference between Fe_{tot} and Fe_{intra} uptake rates.

Molar uptake rates of C were estimated by the following equations: C uptake = (naturally occurring DIC x ^{14}C-POC × 1.05)/(^{14}C-DIC added), with the naturally occurring concentration of DIC = 2,100 µmol L^{-1} and 1.05, the correction for the preferential uptake of light isotopes (Welschmeyer and Lorenzen 1984). Methods for DIC analysis are described in Delille et al. (2014).

Validation of the experimental set-up

The question of time series is of considerable interest in a dynamic environment, especially in such remote places where data collected is unique. In situ (Day 26 and 32) and shipboard (Day 6 and 29) incubations were alternated during ISPOL to maximize our stay (note that the amount of time spent by science expeditioners on sea ice was restricted by worsening sea-ice conditions). The temperature and light intensity in the ship's culture room were controlled and purposefully set to mimic in situ conditions to ensure the same growing conditions were met. The temperature of the culture room was set at − 1 ± 1 °C. In situ temperatures in bottom sea ice measured using a Testo thermometer varied from − 1.4 to − 1.9 °C (see Tison et al. (2008) for detail). In situ light of 0.5 to 40 µmol m^{-2} s^{-1} was measured at the ice/water interface using a LiCOR sensor positioned at different angles to capture in situ irradiance. Using the same sensor, light measured in the ship's culture room varied between 12 and 43 µmol m^{-2} s^{-1} depending on the distance of the radio-labelled petri dish from the light source. Hence, we are confident that our experiments adequately reproduced natural light conditions.

$$^{55}Fe\,on\,filter = \frac{(cpm\,on\,filter\,sample - cpm\,on\,filter\,control)}{^{55}Fe\,specific\,activity} \times \frac{1}{counting\,efficiency},$$

Statistical analysis

Key environmental sea-ice parameters such as in situ temperature, salinity, sea-ice thickness, and DFe, Chl a, and POC concentrations were log transformed and assessed for correlations with Fe uptake using Pearson correlation analysis. Transformed data were normally distributed according to the Shapiro–Wilk test.

Results

Background physical and biogeochemical variables

Detailed sea-ice thermodynamics, chemical properties and microbial diversity of the ISPOL drifting station are presented in Lannuzel et al. (2008), Lannuzel et al. (2013), and Tison et al. (2008), respectively. Sea-ice thickness at the chosen site remained stable between sampling days. Radiation and weather conditions (at 5-min interval) are reported in Nicolaus et al. (2009). To summarize, the visited ice floe was level first-year sea ice 0.8–0.9 m thick. In situ ice temperatures were above − 5 °C and showed clear signs of warm "spring–summer" transition regime (Tison et al. 2008).

Time series at the sea ice/seawater interface

The sharp decrease in DFe concentrations in bottom sea ice within the first 10 days (Fig. 2a) and the general DFe increase in underlying seawater (Fig. 2b) was indicative of Fe fertilization of seawater from melting sea ice (Lannuzel et al. 2008). During the time of the ISPOL study, POC concentrations in bottom sea ice deviated by 20% on average and ranged from 265 to 470 µmol C L^{-1} (Fig. 2c). POC concentrations nearly doubled in seawater underneath but only ranged between 2.8 and 5.7 µmol C L^{-1} (Fig. 2d). Seawater Chl a remained far lower than the sea-ice Chl a values but increased by more than 4 times during the survey (0.03 to 0.14 µg L^{-1}, Fig. 2d).

This point was further explored by looking at the biomass distribution in the different compartments and how autotrophs and heterotrophs abundances evolved over time. A full description of the communities is presented in Lannuzel et al. (2013), but briefly, autotrophs represented on average 82 ± 16% (n = 7) of the total biomass in sea ice and vastly dominated in top (90 ± 7%) and bottom (96 ± 7%) sea ice (Fig. 3). By contrast, autotrophs only represented 41 ± 13% ($n = 7$) of the total biomass in seawater, with contribution from each group changing between the start and end of the survey. Therefore, autotrophs and heterotrophs—in particular heterotrophic bacteria and protozoa – contributed equally to the total biomass in under-ice seawater (Fig. 3c). Figure 3 also clearly shows that top and bottom sea ice hosted very different types of organisms. For instance, *Phaeocystis* single cells (Prymnesiophyte) dominated the top sea ice (Fig. 3a), whilst bottom sea ice was almost solely colonized by pennate diatoms (Fig. 3b). Despite a slight change in POC concentrations (Fig. 2c),

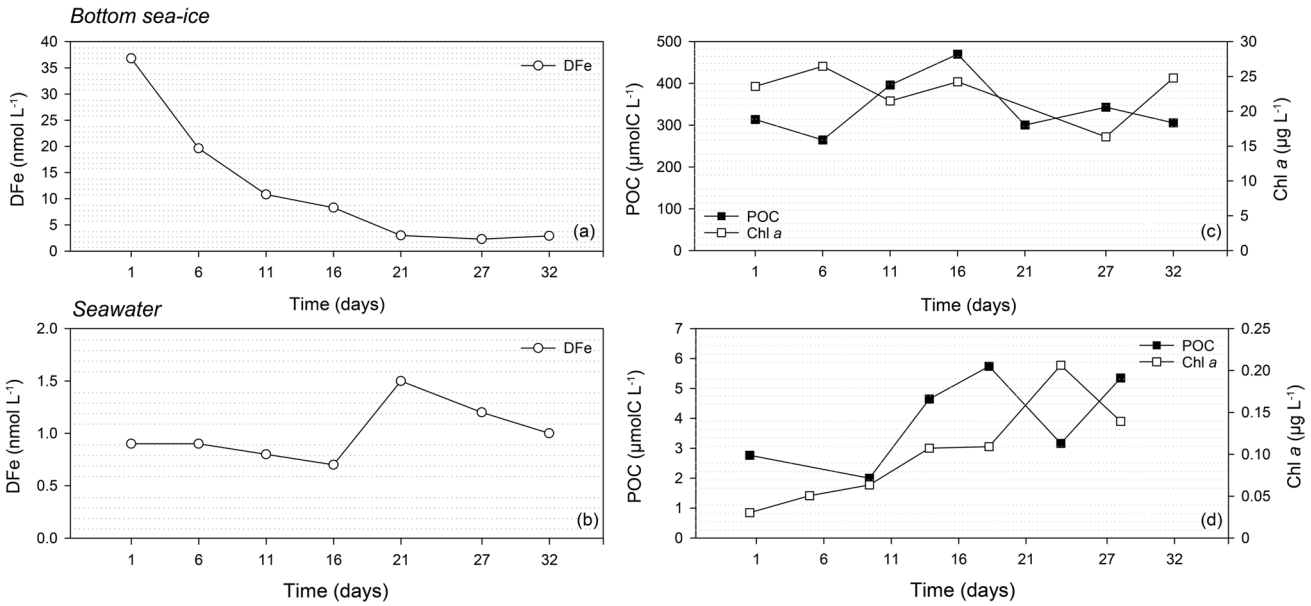

Fig. 2 Bulk concentrations of dissolved iron (DFe, nmol Fe L^{-1}), particulate organic carbon (POC, µmol C L^{-1}), and chlorophyll a (Chl a, µg L^{-1}) in (**a**, **c**) bottom sea-ice Sects. (5–10-cm thick, from the bottom of ice cores 0.8–0.9 m long) and (**b**, **d**) underneath seawater (at the interface with sea ice) during the time series. Day 1 represents the day of arrival on site and first day of sampling. Data are from Lannuzel et al. (2008)

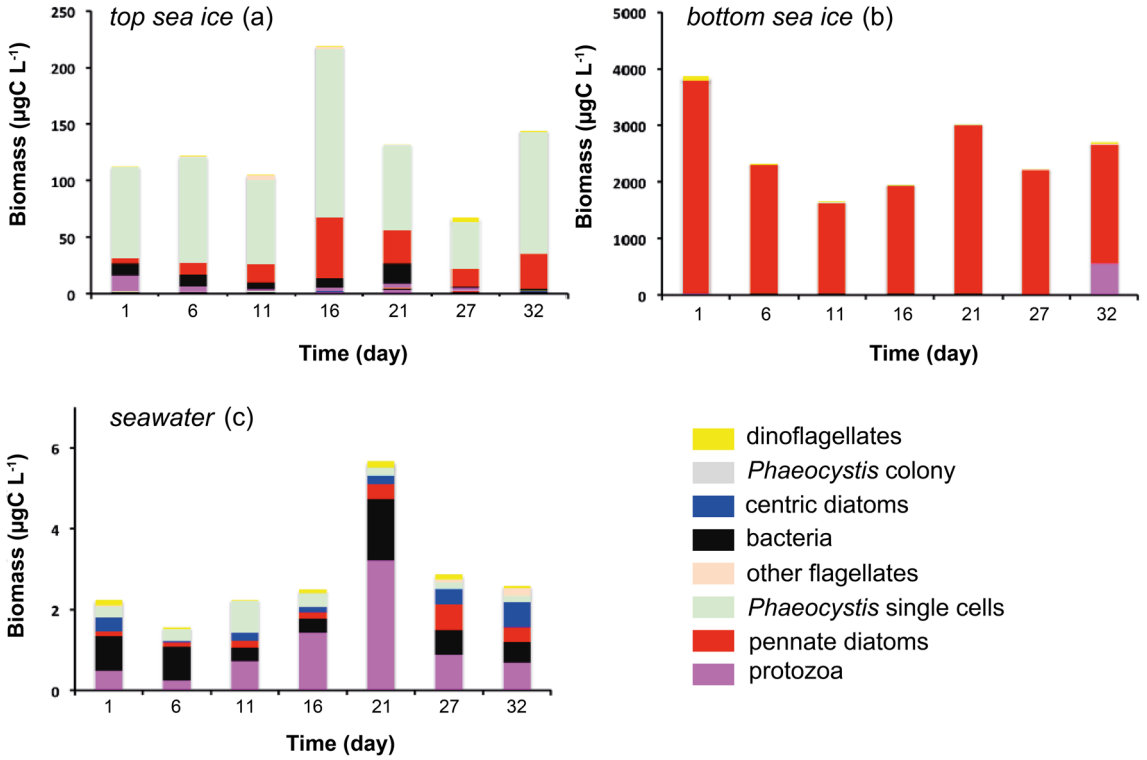

Fig. 3 Biomass distribution of autotrophs, protozoa, and bacteria during the ISPOL time series. Data are presented for samples of **a** top sea ice (uppermost 6-cm sections of ice cores), **b** bottom sea ice (6-cm sections from ice cores 0.8–0.9 m long), and **c** under-ice seawater, at the ice/water interface. Data from Lannuzel et al. (2013)

the contribution of each group to carbon biomass remained fairly stable in sea ice over time.

Bulk iron uptake rates and contribution of different size fractions

Intracellular Fe uptake rates from the bulk community (> 0.8 µm) and two size classes (0.8–10 µm and > 10 µm) obtained from the incubations of bottom sea ice, slush, and seawater are presented in Fig. 4. In bottom sea ice, Fe_{intra} increased from 5.8 to 194 pmol Fe L^{-1} d^{-1} with the lowest and highest values measured on Day 6 and Day 32, respectively. The bottom sea-ice community was composed by more than 90% of autotrophs, specifically pennate diatoms (Fig. 3b). Diatoms range in size from a few µm to up to several hundred µm. Large cells (> 10 µm) were the main contributor to Fe_{intra} uptake at the start of the survey. Small autotrophs (0.8–10 µm) were present in bottom sea ice on

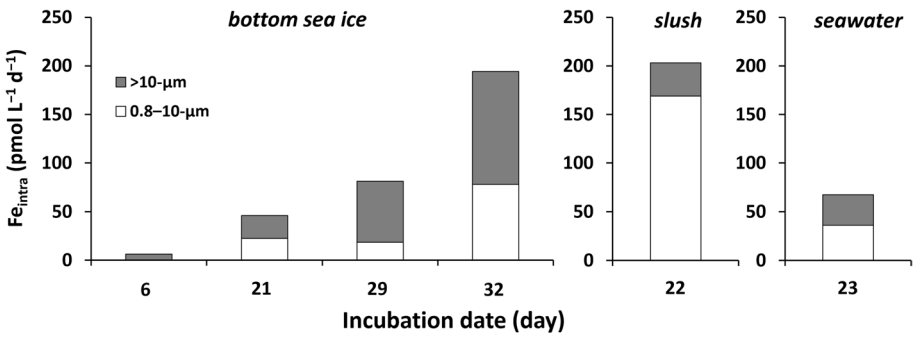

Fig. 4 Intracellular ^{55}Fe uptake rates in bottom sea ice, slush, and under-ice seawater samples. Short-term ^{55}Fe incubations were performed on 1-cm-thick bottom sea-ice sections under temperature-controlled laboratory conditions (Day 6 and Day 29) or in situ conditions (Day 21 and Day 32). Slush (Day 22) and under-ice seawater (Day 23) were incubated under temperature-controlled laboratory conditions. White bars indicate Fe_{intra} uptake by the 0.8–10-µm size fraction and grey bars indicate Fe_{intra} uptake measured on 10-µm filters

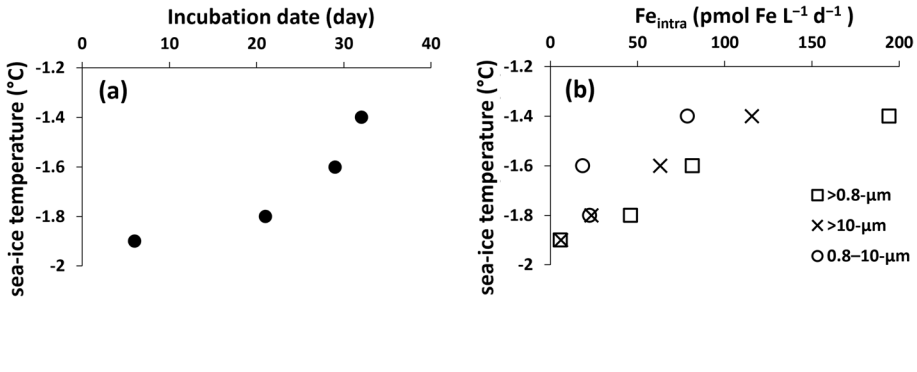

Fig. 5 a Temporal warming of bottom sea ice and **b** Fe_{intra} uptake rates from the bulk community (> 0.8 µm) and two size classes of algae (0.8–10 µm and > 10 µm) plotted against sea-ice temperatures

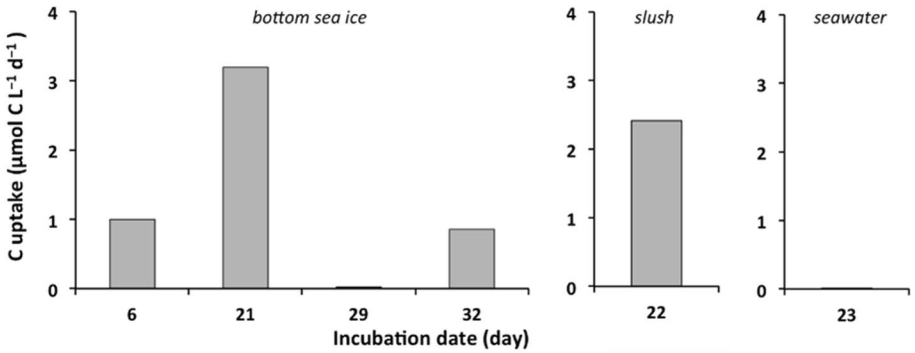

Fig. 6 ^{14}C uptake rates in bottom sea-ice, slush, and under-ice seawater samples. Short-term ^{14}C incubations were performed on 1-cm-thick bottom sea-ice sections under temperature-controlled laboratory conditions (Day 6 and Day 29) or in situ conditions (Day 21 and Day 32). Slush (Day 22) and under-ice seawater (Day 23) were incubated onboard the ship. The bar for under-ice seawater indicates the lowest of the ^{14}C uptake rates measured (0.003 µmol C L^{-1} d^{-1}) compared to the bottom sea-ice and slush samples (0.03–3.19 µmol C L^{-1} d^{-1})

Day 6 (Lannuzel et al. 2013) but their contribution to Fe_{intra} uptake was negligible (Fig. 4). On Day 21, the contribution of small cells to Fe_{intra} went up to 49%, then 23% on Day 29, and finally increased again to 40% by Day 32. Overall Fe_{intra} for the whole community (> 0.8 µm) increased by more than 30 times between Day 6 and Day 32 (Fig. 4), whilst the total carbon biomass remained stable (Fig. 2c).

A positive and significant correlation between sea-ice temperature and Fe_{intra} uptake rates for both small (0.8–10 µm) and large (> 10 µm) cells (Fig. 5b; Pearson correlations: $r = 0.893$, $p = 0.107$, $n = 4$ and $r = 0.996$, $p = 0.004$, $n = 4$, respectively), although the confidence level for small cells was < 90%.

Measured C and Fe:C uptake rates

In situ C uptake rates in bottom sea ice ranged between 0.03 and 3.19 µmol C L^{-1} d^{-1} (Fig. 6). We measured a wide range of Fe_{intra}:C uptake ratios in bottom sea ice, from 5.8-µmol Fe mol^{-1} C on Day 6 to up to 230-µmol Fe mol^{-1} C on Day 32 (Fig. 7a). One outlier value of 3,100 µmol Fe mol^{-1} C was measured for Day 29 and likely due to an extremely low ^{14}C uptake (0.03 µmol C L^{-1} d^{-1}) compared to other sampling days.

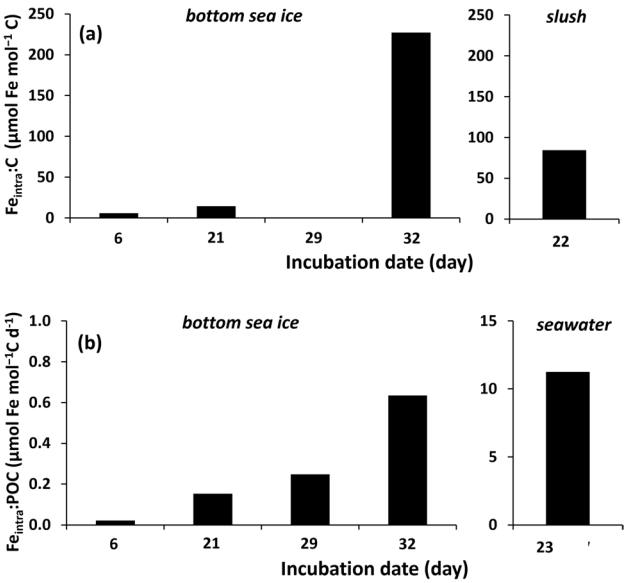

Fig. 7 Ratios of **a** Fe_{intra} uptake to ^{14}C uptake and **b** Fe_{intra} uptake to POC concentration. The uptake ratios in **a** do not include values for bottom sea ice on Day 29 or under-ice seawater on Day 23 due to extremely low values for ^{14}C uptake measured in those samples (Fig. 6). Ratios of Fe_{intra} uptake to POC concentration in **b** do not include a ratio for slush because POC in slush was not measured

In slush, C uptake on day 22 was 2.4 µmol C L^{-1} d^{-1} and within the range of the bottom sea-ice values (Fig. 6). The Fe_{intra}:C uptake ratio was 84.0 µmol Fe mol^{-1} C and sat within the ranges observed for bottom sea ice (Fig. 7a).

By contrast, seawater exhibited an extremely low C uptake (0.003 µmol C L^{-1} d^{-1}, Fig. 6), resulting in unrealistically high Fe_{intra}:C uptake ratio (24,000 µmol Fe mol^{-1} C).

Intracellular versus extracellular Fe

Data on Fe_{tot} and Fe_{intra} by microorganisms are compiled in Table 3. In our study, Fe_{tot} and Fe_{intra} in bottom ice were measured on days 6, 21, 29, and 32 of the time series. Fe_{tot} and Fe_{intra} in slush and seawater were measured on days 22 and 23, respectively. Fe_{intra} represented only 1% of the Fe_{tot} in slush, whilst Fe_{intra} reached 8% of Fe_{tot} in seawater. Fe_{intra} in bottom sea ice sat between the slush and seawater values, with Fe_{intra} = 1–7% of the Fe_{tot} uptake. Therefore, regardless of the type of sample, more than 90% of Fe was bound to the outside of the cells.

Discussion

Caveats and compromises in the sampling design

Sea ice, like sediment and soil, is a heterogeneous medium. Adjacent sea-ice cores may have different physical,

Table 3 Comparison of intracellular (Fe_{intra}) and total (Fe_{tot}) Fe uptake rates and Fe:C uptake ratios in sea-ice and associated environments.

Sample type and location (project acronym)	Fe_{intra} uptake (pmol L^{-1} d^{-1})	Fe_{tot} uptake (pmol L^{-1} d^{-1})	Fe_{intra}:C uptake ratio (µmol mol^{-1})	Fe_{tot}:C uptake ratio (µmol mol^{-1})	Reference
Antarctic sea ice					
Bottom sea ice (n = 4)	6–194	157–4,591	5.8–230[a]	157–3,030[b]	This study
Under-ice seawater (n = 1)	68	830	na[c]	na[d]	This study
Slush (n = 1)	201	23,850	84	9,900	This study
Southern Ocean seawater					
Drake passage	na	na	3.0–14.3	na	Hopkinson et al. (2013)
HNLC[e]—south of Australia	na	na	7–49	na	Tovar-Sanchez et al. (2003)
Kerguelen Plateau[f] (KEOPS)	4.4–6.2	na	na	na	Sarthou et al. (2008)
Kerguelen Plateau[f] (KEOPSII)	19–40	na	3.7–22.9	na	Fourquez et al (2015)
Sub-Antarctic zone	90–193	na	na	na	Fourquez et al. (2020)
Sub-Antarctic zone	11–27	na	6.6	na	Ellwood et al. (2020)
South of Australia (SOIREE[g])	3.07–11.9	na	2.7–3	na	Bowie et al. (2001)
HNLC waters of New Zealand (FeCycle)	26.2–101	na	2–19	na	Strzepek et al. (2005)
			4–12.5	na	Frew et al. (2006)
		na	5–20	na	McKay et al. (2005)
HNLC waters of New Zealand (FeCycleII)	na	na	na	1.2–33.3	King et al. (2012)
Unfertilized HNLC waters (SOFEX[g])	na	na	na	6.2–14.3	Twining et al. (2004)
Fe-fertilized HNLC waters (SOFEX[g])	na	na		10–40	Twining et al. (2004)
Laboratory phytoplankton cultures					
Fe limited	na	na	0.6–14	na	Maldonado and Price (1996)
Fe replete	na	na	26–102	na	Maldonado and Price (1996)
	na	na	2.3–370	na	Sarthou et al. (2005)
	na	na	6–500	na	Sunda and Huntsman (1997)
		na	0.4–8.6	na	Strzepek et al. (2011)

Results are reported for this study, other field-based studies in natural and Fe-fertilized surface waters from the Southern Ocean as well as laboratory-based phytoplankton cultures

[a]Ratio of 3,150 in bottom sea ice on Day 29 was excluded from this range due to extremely low ^{14}C uptake

[b]Ratio of 180,000 in bottom sea ice on Day 29 was excluded from this range due to extremely low ^{14}C uptake

[c]na indicates not available; ratio of 23,700 in seawater was excluded from this range due to extremely low ^{14}C uptake

[d]Ratio of 290,000 in seawater was excluded from this range due to extremely low ^{14}C uptake

[e]High nutrient low chlorophyll

[f]Naturally Fe-fertilized areas

[g]Artificially Fe-fertilized field experiments

chemical, and biological compositions and obtaining a sampling programme representative of the sea-ice system is therefore challenging (Miller et al. 2015). Ideally, replicate samples should be collected for each variable considered. The horizontal patchiness of sea-ice algae has been mainly attributed to the spatial variability in physical sea-ice properties (Eicken et al. 1991) and light exposure (Raymond et al. 2009). To keep processes as simple as possible for post-cruise data interpretation and modelling, the ISPOL "clean site" (Tison et al. 2008) was chosen to be flat (no ridging), unflooded, first-year sea ice. The 14 cores (one core per variable) collected on each sampling day were 90 cm thick, of same ice texture and snow thickness, and sampled within a 2.5×5 m area. The small size of the area minimizes heterogeneity between the cores to allow a multidisciplinary understanding of the physical, biological, and biogeochemical processes at play. Collecting replicate cores for each variable would increase the size of the area and increase the likelihood for the increased distance between the ice cores to adversely affect data interpretation. The experiments presented here are also time sensitive. Adding more replicates would affect the incubation time, as time dedicated to each step of the process described below would triple. We therefore chose to collect one replicate per variable for a whole suite of variables rather than replicate cores for a limited set of variables. Consequently, all the results presented here are single measurements and do not bear standard deviations.

Autotrophic versus heterotrophic contribution to Fe uptake

When sea ice melts, DFe is released first together with salts and DOC, whilst particulate Fe is released later together with the dense brines and POC (Lannuzel et al. 2013). Autotrophs vastly dominate in bottom sea ice but heterotrophs represent up to 50% of the biomass in seawater. Therefore, does the Fe supplied by melting sea ice stimulate the seawater microbial community and if so, which type of organisms (heterotrophs versus autotrophs) benefit the most from this fertilization? Comparing Fe_{intra}: C uptake ratios and Fe_{intra}: POC ratios in both sea ice and seawater may help answer these questions by deciphering the autotrophic from heterotrophic activities.

As a first approach, we compared Fe_{intra} in bottom sea ice with measurements in slush and seawater. In slush, Fe_{intra} uptake by the bulk community was measured once on Day 22 and similar to bottom sea ice on Day 32 (Fig. 4), with small cells (0.8–10 µm) contributing more than 80%. Both autotrophs and heterotrophs cells were likely present at the time of sampling in slush, similar to what was found in top sea ice (Fig. 3a) (Lannuzel et al. 2013). In seawater, Fe_{intra} by the bulk community was within range of the sea-ice values, and with small and large cells contributed equally to Fe_{intra} (46 and 54% for > 10 µm and 0.8–10 µm, respectively).

The short-term (5–6 h) nature of the incubation minimizes radiocarbon losses by respiration (Schoemann et al. 2001). Rates of inorganic C uptake during our experiments can therefore be used to evaluate the proportion of autotrophic activities in relation to Fe_{intra} uptake by the bulk community. The ^{14}C uptake rates measured in bottom sea ice are indicative of algal growth, since autotrophic algae (pennate diatoms) represented 96 ± 7% of the total biomass in these samples (Fig. 3b). Therefore, when normalized to ^{14}C uptake, Fe_{intra}:C uptake ratios can act as indicators of Fe uptake in relation to algal growth.

The extremely low C uptake and high Fe_{intra}:C uptake ratio observed in seawater may be partly explained by large differences in biomasses (Fig. 3c) and/or that autotrophic cells were not involved in Fe uptake. To account for the lower contribution of autotrophs to the carbon biomass in seawater compared to bottom sea ice, Fe_{intra} uptake rates in seawater were also normalized to POC concentrations (Fig. 7b). We note that Fe_{intra}:POC by the bulk community (> 0.8 µm) was in fact an order of magnitude higher in seawater than in bottom sea ice (Fig. 7b).

Collectively, these results suggest that heterotrophs were responsible for most of the Fe uptake in seawater, as opposed to slush and bottom sea-ice environments where autotrophs dominated. Another non-exclusive explanation is that phytoplankton in seawater was mixotroph (shared ability to use inorganic and organic sources of carbon), making it is impossible to distinguish which organisms contributed the most to Fe uptake.

Comparison to previous studies

The Fe_{intra} measured in under-ice seawater is within the range of previous field studies, although on the high end (Table 3). Over 90% of the ^{55}Fe taken up by the particles was adsorbed to the cell surfaces, regardless of the type of sea-ice environment incubated. As a comparison, the oxalate wash used to distinguish between scavenged and intracellular Fe in suspended particles collected in the SO showed that 60–80% of the total Fe associated with these samples was found to be surface-adsorbed, i.e. not intracellular (Tovar-Sanchez et al. 2003). Frew et al. (2006) reported that around 45% of particulate Fe (PFe) was removed by the oxalate wash and could be classified as "extracellular" in sub-Antarctic waters South of New Zealand. Although we used a Ti- EDTA wash and not an oxalate wash, the two approaches have been shown to give comparable results (Tang and Morel 2006; Fourquez et al. 2012). Like our study, the Southern Ocean Iron Experiment (SOFeX) experiments used ^{55}Fe incubations and Ti-EDTA washes (Twining et al. 2004). They report

that 20–84% of the Fe was externally bound, depending on the size of the particles. The extremely high fraction of Fe adsorbed to marine particles in the sea-ice environment may be due to exopolysaccharides (EPS). EPS are gel-like substances produced by algae and bacteria. Sea ice is particularly enriched in EPS relative to ice-free seawaters (van der Merwe et al. 2009; Krembs et al. 2011; Ewert and Deming 2011). Their stickiness and negatively charged surfaces (Decho 1990; Underwood et al. 2010) possibly allow EPS to bind metallic cations (Croot and Johansson 2000; Verdugo et al. 2004), such as Fe^{2+} and Fe^{3+} in sea ice (Lannuzel et al. 2015). The complexation of Fe with EPS would explain the extremely high fraction of Fe attached to the outside of the particles, especially within the slush and bottom ice samples where EPS are likely in higher proportions relative to under-ice seawater.

The upper values for in situ carbon assimilation in bottom sea-ice samples exceeded ranges previously reported from in situ measurements in newly formed Antarctic sea ice in the Weddell Sea in autumn (Mock 2002) and bottom pack ice from the East Antarctic sector in spring (Roukaerts et al. 2015). Daylength and light intensity Chl a concentration and temperatures were all lower in Mock's study, potentially leading to the lower C uptake rates their autumn visit compared to our summertime study. Similarly, the shorter photoperiod and thicker snow cover (0.3 to 0.8 m) experienced in early spring in Roukaert's study reduced light penetration through the sea-ice cover and explain their lower ^{14}C uptake rates compared to our summertime series where photoperiod was longer and snow only reached about 0.06 to 0.25 m in thickness (Tison et al. 2008). In slush, the C uptake rate was within the range of the bottom sea-ice values (Fig. 5). Seawater exhibited extremely low C uptake (Fig. 5) compared to the incubated bottom sea-ice and slush samples. Tortell et al. (2013) measured much higher averaged maximum ^{14}C fixation rates in austral summer in slush, sea ice, and in under-ice seawater. The lack of seawater replicates in our study does not allow strong conclusions. However, one could expect that autotrophs may have adopted a mixotrophic behaviour to sustain their growth in this extremely low light environment. Mixotrophy may be an important trophic mode that is currently overlooked in the Antarctic ecosystem. More investigation is needed to confirm or refute this result.

The Fe_{intra}:C uptake ratios measured in bottom sea ice are either within range reported for Fe-replete phytoplankton cultures or considerably higher than the ranges reported in Fe-fertilized areas (open ocean) of the SO (Table 3). Autotrophs largely dominate in bottom sea ice, and Fe_{intra}:C uptake ratios are therefore indicative of the amount of Fe needed for autotrophic activities. In slush and under-ice seawater, where heterotrophs and autotrophs are equally abundant, it is more appropriate to estimate Fe uptake normalized to POC biomass rather than ^{14}C uptake. The Fe_{intra}:POC ratio in seawater (11.2 µmol Fe mol^{-1} C d^{-1}) sits at the upper end of the range of Fe_{intra}:POC ratio values reported for sub-Antarctic waters near Kerguelen Island during the KEOPS2 spring bloom (Fourquez et al. 2015). Our work needs to be repeated and replicates recorded to allow better comparison between under-ice seawater and open ocean studies.

Extracellular scavenging as a Fe uptake strategy by sea-ice algae

Regardless of cell size, our results are by far the highest rate of scavenged Fe so far measured in oceanic samples. Enhanced adsorption of cellular Fe to the outside of the phytoplankton cells was observed following Fe fertilization during SOFeX (Twining et al. 2004). The accumulation of Fe on the direct surroundings of the cells could be aided by the presence of ligands in sea ice and more specifically EPS, which have been shown to control DFe concentrations in this environment (Lannuzel et al. 2015; Genovese et al. 2018) and increase Fe bioavailability (Hassler et al. 2011). Ligands ultimately maintain Fe in solution for longer than would otherwise occur, thereby delaying the adsorption of DFe onto particles and increasing the residence time of bioavailable forms of Fe.

From a biogeochemical perspective (i.e. cycling and fate of an element), such high Fe fraction bound to the outside of the cells may be considered as luxury uptake. The luxury uptake mechanism is a process during which cells accumulate excess Fe, sometimes at concentrations up to 30 times higher than the Fe levels required for growth (Sunda and Huntsman 2011). This Fe storage strategy would be especially useful in environments like sea ice where Fe is ephemerally available (Marchetti et al. 2009). Diatoms, which are the most abundant phytoplankton groups in bottom sea ice (Fig. 3b), are especially well adapted to this strategy (Twining et al. 2021). Alternatively, the high fraction of Fe bound to the outside of the cells could illustrate an experimental bias. We did not correct for background radioactivity on the filters (^{55}Fe adsorbed onto the filter and/or onto particles that are not efficiently removed by the Ti-EDTA wash solution). Abiotic sorption of ^{55}Fe to the filters may contribute to the extremely high Fe_{tot} uptake values.

Effects of environmental conditions on Fe uptake by natural sea-ice communities

Sea-ice habitats are often characterized by steep gradients in temperature, CO_2, salinity, irradiance, and other environmental factors. Organisms inhabiting the pack ice can

be subject to very low irradiance or even periods of complete darkness during wintertime, which will considerably alter the development of autotrophic species in favour of heterotrophic processes (Garrison and Close 1993). Low temperatures constrain metabolic rates and cellular growth requirements that are intrinsically linked to the Fe demand by organisms (Strzepek et al. 2011). To explore whether such environmental factors could explain the higher Fe uptake rate observed in bottom sea ice on Day 32 compared to Day 6, we tested for correlation between the Fe uptake and environmental sea-ice DFe concentration and temperature.

Effect of temperature

A correlation between Fe_{intra} uptake rate and sea-ice temperature is observed (Fig. 5b). The warming over the course of our sampling period is however too small (+0.5 °C, Fig. 5a) to explain the fourfold Fe_{intra} uptake by large sea-ice diatoms between Day 6 and Day 32 (Fig. 4b). Iron plays a pivotal role in enzymatic reactions that are sensitive to temperature (Raven and Geider 1988), such as photosynthesis and nitrogen transport. Synergistic effects of an increase in DFe concentration (by + 1 nmol L^{-1}) and increase in temperature (by + 4 °C) have been observed previously on phytoplankton assemblages in the Ross Sea, Antarctica (Rose et al. 2009), where simultaneous increases in both factors magnified rate increases over single-factor treatments by 8–16 times. More generally, when microorganisms at temperatures suboptimal for growth, particularly sub-zero temperatures, experience a temperature increase of only a few degrees, the effect on some transport rates can be unexpected (Jumars et al. 1993; Berges et al. 2002), including Q10 values > 12 compared to the typical value of 2 (Yager and Deming 1999). We suggest that laboratory-based experiments on the combined effect of stressors (e.g. Fe, types of ligands, light, temperature, and macro-nutrients) on Antarctic sea-ice algae and bacteria are needed to understand how sub-zero temperatures constrain Fe_{intra} uptake rates.

Effect of DFe concentration

Iron-deplete phytoplankton have been shown to transport Fe into the cell at a faster rate than Fe-replete cells (Harrison and Morel 1986). Low Fe concentrations are thought to induce upregulation of the number of cell-surface Fe transport systems, resulting in considerably faster Fe uptake rates (Hudson and Morel 1990; Taylor et al. 2013). This upregulation of cellular Fe acquisition machinery has been observed in a SO eddy system, with a higher Fe:C uptake ratio inside the eddy (Fe limited) than outside the eddy (Fe replete) (Ellwood et al. 2020). In our study, in situ DFe concentrations were high (3.1–20.4 nmol L^{-1}) and can be considered Fe replete. No significant correlation between DFe concentration and cellular Fe uptake was observed. These experiments should be repeated over a gradient of low to high sea-ice DFe concentrations to confirm or refute the hypothesis that decreasing sea-ice DFe concentration may lead to an increase in biological Fe uptake by sea-ice communities.

Trends in Fe:C uptake ratios

Sea ice

Sympagic ice algae are the most abundant in the ice/water interface. They often grow under low light and consume macro-nutrients from the underlying seawater, with micronutrient Fe supplied from the sea-ice brine system. Our measurements of Fe_{intra}:C uptake ratios (µmol Fe mol^{-1} C) in bottom sea-ice varied by two orders of magnitude between sampling days. This variability was mainly driven by Fe rather than C uptake, which is also illustrated by increased Fe_{intra}:POC ratio over time, whilst biomass remained relatively stable. In the meantime, the contribution of small cells (0.8–10 µm) to bulk Fe_{intra} uptake (> 0.8 µm) overall increased between Day 6 and Day 32. Hence, we believe that this result illustrates the change in bottom sea ice from a dominance of large diatoms at the start of the experiments to a mixture of small and large diatoms as summer progresses and DFe concentrations in bottom sea ice decrease. In general, smaller cells have a clear advantage in accessing DFe because of their high surface area-to-volume ratios (Lis et al. 2015). Large diatoms require higher more DFe than smaller diatoms (Timmermans et al. 2004), but that does not necessarily translate into higher Fe_{intra}:C (Strzepek et al. 2011) in larger than smaller cells. A negative correlation between cellular Fe:C content and cell biovolumes has been reported in several SO studies, both in situ (Twining et al. 2004) and in the laboratory (Sunda and Huntsman 1995, 1997; Strzepek et al. 2011). The shift between large and small diatom species could easily influence Fe_{intra}:C uptake ratios, as well as how much and under which form Fe is released into seawater when sea ice melts.

Seawater and slush

Since POC and Chl a concentrations in bottom sea ice were stable over time (Fig. 2c), the POC and Chl a increase in seawater is likely a signature of phytoplankton growth as a response to Fe fertilization, rather than due to the release of ice algae from bottom sea ice. Seawater communities are exposed to low irradiance but benefits from high macronutrients and Fe released from melting sea ice. During the ISPOL time series, autotrophic organisms (mostly *Phaeocystis*) represented only 41 ± 13% of the total biomass in seawater (Lannuzel et al. 2013). Bacteria dominated in

under-ice seawater until Day 11 and then protozoa dominated in terms of biomass (Fig. 3c). The dominance of heterotrophs in under-ice seawater can be explained by very low irradiance (and even complete darkness periods during wintertime), which considerably alters the development of autotrophic species in favour of heterotrophic processes (Garrison and Close 1993). Moreover, Sunda and Huntsman (2011) observed an increased in cellular Fe:C ratio when light availability is low. Their result matches those from our under-ice seawater incubation experiment, where the Fe_{intra}:POC was in fact an order of magnitude higher in seawater than in bottom sea ice (Fig. 7b). These results suggest that heterotrophs were responsible for most of the Fe uptake in seawater, as opposed to bottom sea ice where autotrophs dominated. Heterotrophic bacteria have historically been considered strong competitors against phytoplankton for access to Fe (Tortell et al. 1996; Maldonado and Price 1999). However, recent studies have challenged this view and new concepts have emerged (Fourquez et al. 2020; 2022). We recommend future work using laboratory-based cultures of phytoplankton (strict autotrophs and mixotrophs) and heterotrophic bacteria to unravel these questions. The development of culture collection such as the freely accessible Antarctic Bacterial Culture Collection (https://zenodo.org/record/5763724) would support these efforts.

An algal community at the ice/snow interface may have optimal irradiance for growth but is often restricted by nutrient supply. The infiltration of seawater and/or seawater flooding events in the snowpack result in slush formation; this process can provide additional macro-nutrients from seawater to induce algal development in slush (e.g. Arrigo et al. 1997; Thomas and Dieckmann 2002). This nutrient supply, together with high irradiance and DFe concentrations (2.2 nmol L^{-1}), might stimulate the biological drawdown of DFe in slush. Such stimulation is supported by our incubation experiments with slush sampled on Day 22, when a high Fe_{intra} uptake rate was observed (203 pmol Fe L^{-1} d^{-1}). This Fe_{intra} uptake rate in the slush is similar to the highest Fe_{intra} uptake rate measured in the bottom sea-ice samples on Day 32 (194 pmol Fe L^{-1} d^{-1}). Unlike the bottom ice assemblage where large diatoms dominated, the small size fraction (0.8–10 µm) contributed to over 80% of the Fe_{intra} uptake in the slush sample. Although no samples were collected to confirm this suggestion, the slush community was most likely colonized by *Phaeocystis*, as single cells, that dominated in terms of biomass and abundance in the top sea-ice samples collected during the time series (Fig. 3a).

Is the decrease of DFe concentration in bottom sea ice due to brine drainage or biological uptake?

The ISPOL Fe time series study carried out in the western Weddell pack ice during spring–summer demonstrated a marked decrease of the initial DFe stock in sea ice over a 32-day period, especially in bottom sea ice (Fig. 2a). This decrease was mirrored by an increase in Fe_{intra} uptake in bottom sea ice (Fig. 4). This finding begs the question: was DFe lost through brine drainage or biological uptake? Using the maximum Fe_{intra} uptake rate of 194 pmol Fe L^{-1} d^{-1} measured in bottom sea ice, we estimated that it would take 5 months for sea-ice algae to exhaust the stock of DFe. Our data coupled with the increase in DFe concentration in the under-ice water column, therefore support the previous hypothesis that the decrease in DFe concentration witnessed in sea ice during the ISPOL time series was due primarily to brine drainage (Lannuzel et al. 2008), not biological uptake.

Conclusion

This study is the first to describe the dynamics of biological Fe uptake in the sea-ice environment. Our results point towards to several key considerations for the polar biogeochemical community. Intracellular Fe uptake rates, both absolute and normalized to C uptake and POC, are highly variable in space and time during the melting season, with the slush and under-ice seawater showing the highest and the lowest Fe_{intra} uptake rates, respectively. The range of Fe_{intra} uptake rates by sea-ice algae (6–194 pmol Fe L^{-1} d^{-1}) however extends to higher values than those reported in Fe-rich sub-Antarctic surface waters. The most striking result from our experiments is the overconsumption of Fe relative to C assimilation by sea-ice diatoms. The fourfold increase in the Fe_{intra}: C uptake ratio is likely due to enhanced uptake by small diatoms as the season progressed. > 90% of the total uptake of Fe in our samples was not intracellular; this result highlights the need for modellers to account for extracellular Fe in the parameterisation of sea-ice biogeochemical models. The extracellular Fe reservoir may be aided by the presence of EPS which act as organic ligands and increase Fe bioavailability. Whilst we cannot assess if this pool of Fe is an extracellular storage mediated by the cells, an indirect effect of the presence of EPS for other purposes (e.g. cryoprotection) or a combination of both processes, our findings do have important biogeochemical and ecosystems implications. Diatoms favour C export and drive biogeochemical fluxes (Buesseler 1998), meaning that the high Fe:C ratio measured in our study may strongly affect upper ocean recycling and export of Fe and C in sea-ice-covered environments. Therefore, we encourage future modelling research—that link Fe and C cycling to changes in sea-ice extent—to consider these new findings to help further improve their predictive capabilities.

Acknowledgements The authors are grateful to the officers and crews of the RV Polarstern for their logistic assistance during Ice Station

POLarstern (ISPOL). We would like to thank the Alfred Wegener Institute, especially Michael Spindler, David Thomas, and Gerhard Dieckmann for allowing us to take part in the ISPOL voyage. We thank Prof Tom Trull as well as the two reviewers for their comments which vastly improved the quality of the manuscript.

Author contributions VS contributed to conception and design.VS, DL, JdJ, BD, and JLT contributed to acquisition of data.DL and MF contributed to analysis and interpretation of data.DL, MF, JdJ, BD, and JLT drafted and revised the article.

Funding Open Access funding enabled and organized by CAUL and its Member Institutions.

Declarations

Competing interest The authors declare they have no competing interest of any kind with this research and the publication of this manuscript.

References

Arrigo KR, Worthen DL, Lizotte MP et al (1997) Primary production in Antarctic sea ice. Science 276:394LP – 397. https://doi.org/10.1126/science.276.5311.394

Arrigo KR, van Dijken GL (2003) Phytoplankton dynamics within 37 Antarctic coastal polynya systems. J Geophys Res 108:3271. https://doi.org/10.1029/2002JC001739

Berges JA, Varela DE, Harrison PJ (2002) Effects of temperature on growth rate, cell composition and nitrogen metabolism in the marine diatom *Thalassiosira pseudonana* (bacillariophyceae). Mar Ecol Prog Ser 225:139–146. https://doi.org/10.3354/meps225139

Blain S, Quéguiner B, Armand L et al (2007) Effect of natural iron fertilization on carbon sequestration in the Southern Ocean. Nature 446:1070–1074. https://doi.org/10.1038/nature05700

Bowie AR, Maldonado MT, Frew RD et al (2001) The fate of added iron during a mesoscale fertilisation experiment in the Southern Ocean. Deep Sea Res Part II 48:2703–2743. https://doi.org/10.1016/S0967-0645(01)00015-7

Boyd PW, Watson AJ, Law CS et al (2000) A mesoscale phytoplankton bloom in the polar Southern Ocean stimulated by iron fertilization. Nature 407:695–702. https://doi.org/10.1038/35037500

Brand LE (1991) Minimum iron requirements of marine phytoplankton and the implications for the biogeochemical control of new production. Limnol Oceanogr 36:1756–1771. https://doi.org/10.4319/lo.1991.36.8.1756

Bruland KW, Rue EL, Smith GJ (2001) Iron and macronutrients in California coastal upwelling regimes: Implications for diatom blooms. Limnol Oceanogr 46:1661–1674

Buesseler KO (1998) The decoupling of production and particulate export in the surface ocean. Global Biogeochem Cycles 12:297–310. https://doi.org/10.1029/97GB03366

Croot PL, Johansson M (2000) Determination of iron speciation by cathodic stripping voltammetry in seawater using the competing ligand 2-(2-Thiazolylazo)-p-cresol (TAC). Electroanalysis 12:565–576. https://doi.org/10.1002/(SICI)1521-4109(200005)12:8

Decho AW (1990) Microbial exopolymer secretions in ocean environments: their role(s) in food webs and marine processes. Oceanography Marine Biol Annual Rev 28:73–153

de Jong J, Schoemann V, Maricq N et al (2013) Iron in land-fast sea ice of McMurdo Sound derived from sediment resuspension and wind-blown dust attributes to primary productivity in the Ross Sea, Antarctica. Mar Chem 157:24–40. https://doi.org/10.1016/j.marchem.2013.07.001

de Jong J, Stammerjohn S, Ackley S et al (2015) Sources and fluxes of dissolved iron in the Bellingshausen Sea (West Antarctica): the importance of sea ice, icebergs and the continental margin. Mar Chem 177:518–535. https://doi.org/10.1016/j.marchem.2015.08.004

Delille B, Vancoppenolle M, Geilfus N-X et al (2014) Southern Ocean CO2 sink: the contribution of the sea-ice. J Geophysical Res: Oceans 119:6340–6355. https://doi.org/10.1002/2014JC009941

Dumont I, Schoemann V, Lannuzel D et al (2009) Distribution and characterization of dissolved and particulate organic matter in Antarctic pack ice. Polar Biol 32:733–750. https://doi.org/10.1007/s00300-008-0577-y

Duprat LPAM, Bigg GR, Wilton DJ (2016) Enhanced Southern Ocean marine productivity due to fertilization by giant icebergs. Nat Geosci 9:219–221. https://doi.org/10.1038/ngeo2633

Eicken H, Lange MA, Dieckmann GS (1991) Spatial variability of sea-ice properties. J Geophys Res 96:603–615

Ellwood MJ, Strzepek RF, Strutton PG et al (2020) Distinct iron cycling in a Southern Ocean eddy. Nat Commun 11:825. https://doi.org/10.1038/s41467-020-14464-0

Ewert M, Deming J (2011) Selective retention in saline ice of extracellular polysaccharides produced by the cold-adapted marine bacterium Colwellia psychrerythraea strain 34H. Ann Glaciol 52(57):111–117. https://doi.org/10.3189/172756411795931868

Fourquez M, Obernosterer I, Blain S (2012) A method for the use of the radiotracer 55Fe for microautoradiography and CARD-FISH of natural bacterial communities. FEMS Microbiol Lett 337:132–139. https://doi.org/10.1111/1574-6968.12022

Fourquez M, Obernosterer I, Davies DM et al (2015) Microbial iron uptake in the naturally fertilized waters in the vicinity of the Kerguelen Islands: phytoplankton–bacteria interactions. Biogeosciences 12:1893–1906. https://doi.org/10.5194/bg-12-1893-2015

Fourquez M, Bressac M, Deppeler SL et al (2020) Microbial competition in the subpolar Southern Ocean: An Fe–C Co-limitation experiment. Front Mar Sci 6:76. https://doi.org/10.3389/fmars.2019.00776

Fourquez M, Strzepek RF, Ellwood MJ et al (2022) Phytoplankton responses to bacterially regenerated iron in a Southern Ocean eddy. Microorganisms 10(8):1655. https://doi.org/10.3390/microorganisms10081655

Frew RD, Hutchins DA, Nodder S et al (2006) Particulate iron dynamics during FeCycle in subantarctic waters southeast of New Zealand. Global Biogeochem Cycles 20:GB1S93. https://doi.org/10.1029/2005GB002558

Garrison D, Close A (1993) Winter ecology of the sea-ice biota in Weddell Sea pack ice. Mar Ecol Prog Ser 96:17–31. https://doi.org/10.3354/meps096017

Genovese C, Grotti M, Pittaluga J et al (2018) Influence of organic complexation on dissolved iron distribution in East Antarctic pack ice. Mar Chem 203:28–37. https://doi.org/10.1016/j.marchem.2018.04.005

Gerringa LJA, Alderkamp A, Laan P et al (2012) Iron from melting glaciers fuels the phytoplankton blooms in Amundsen Sea (Southern Ocean): iron biogeochemistry. Deep Sea Res Part I 71–76:16–31

Gradinger R, Ikavalko J (1998) Organism incorporation into newly forming Arctic sea-ice in the Greenland Sea. J Plankton Res 20:871–886

Harrison GI, Morel FMM (1986) Response of the Marine diatom Thalassiosira-Weissflogii to iron stress. Limnol Oceanogr 31:989–997

Hassler CS, Schoemann V (2009) Discriminating between intra- and extracellular metals using chemical extractions: an update on the case of iron. Limnol Oceanogr Methods 7:479–489. https://doi.org/10.4319/lom.2009.7.479

Hassler CS, Schoemann V, Mancuso Nichols C et al (2011) Saccharides enhance iron bioavailability to Southern Ocean phytoplankton. Proc Natl Acad Sci USA 108:1076–1081. https://doi.org/10.1073/pnas.1010963108

Herraiz-Borreguero L, Lannuzel D, van der Merwe P et al (2016) Large flux of iron from the Amery Ice Shelf marine ice to Prydz Bay, East Antarctica. J Geophys Res: Oceans 121:6009–6020. https://doi.org/10.1002/2016JC011687

Hillebrand H, Dűrselen C-D, Kirschtel D et al (1999) Biovolume calculation for pelagic and benthic microalgae. J Phycol 35:403–424

Hopkinson BM, Seegers B, Hatta M et al (2013) Deep-Sea research II planktonic C: Fe ratios and carrying capacity in the southern drake passage. Deep Sea Res II 90:102–111

Hopwood M (2018) Iron from ice. Nat Geosci 11:462. https://doi.org/10.1038/s41561-018-0167-8

Hudson R, Morel F (1989) Distinguishing between extra-and intracellular iron in marine phytoplankton. Limnol Oceanogr 34:1113–1120. https://doi.org/10.4319/lo.1989.34.6.1113

Hudson RJM, Morel FMM (1990) Iron transport in marine phytoplankton: kinetics of cellular and medium coordination reactions. Limnol Oceanogr 35:1002–1020. https://doi.org/10.4319/lo.1990.35.5.1002

Janssens J, Meiners KM, Tison JL et al (2016) Incorporation of iron and organic matter into young Antarctic sea ice during its initial growth stages. Elementa 4:000123. https://doi.org/10.12952/journal.elementa.000123

Jeffery N, Maltrud ME, Hunke EC et al (2020) Investigating controls on sea-ice algal production using E3SMv1.1-BGC. Ann Glaciol 61:51–72. https://doi.org/10.1017/aog.2020.7

Jumars P, Deming J, Hill P et al (1993) Physical constraints on marine osmotrophy in an optimal foraging context. Mar Microb Food Webs 7:121–161

King AL, Sañudo-Wilhelmy SA, Boyd PW et al (2012) A comparison of biogenic iron quotas during a diatom spring bloom using multiple approaches. Biogeosciences 9:667–687. https://doi.org/10.5194/bg-9-667-2012

Krembs C, Eicken H, Deming JW (2011) Exopolymer alteration of physical properties of sea ice and implications for ice habitability and biogeochemistry in a warmer Arctic. PNAS 108(9):3653–3658. https://doi.org/10.1073/pnas.1100701108

Lancelot C, de Montety A, Goosse H et al (2009) Spatial distribution of the iron supply to phytoplankton in the Southern Ocean: a model study. Biogeosciences 6:2861–2878. https://doi.org/10.5194/bg-6-2861-2009

Lannuzel D, de Jong J, Schoemann V et al (2006) Development of a sampling and flow injection analysis technique for iron determination in the sea-ice environment. Anal Chim Acta 556:476–483. https://doi.org/10.1016/j.aca.2005.09.059

Lannuzel D, Schoemann V, de Jong J et al (2007) Distribution and biogeochemical behaviour of iron in the East Antarctic sea ice. Mar Chem 106:18–32. https://doi.org/10.1016/j.marchem.2006.06.010

Lannuzel D, Schoemann V, de Jong J et al (2008) Iron study during a time series in the Western Weddell pack ice. Mar Chem 108:85–95. https://doi.org/10.1016/j.marchem.2007.10.006

Lannuzel D, Schoemann V, Dumont I et al (2013) Effect of melting Antarctic sea ice on the fate of microbial communities studied in microcosms. Polar Biol 36:1483–1497. https://doi.org/10.1007/s00300-013-1368-7

Lannuzel D, Grotti M, Abelmoschi ML et al (2015) Organic ligands control the concentrations of dissolved iron in Antarctic sea ice. Mar Chem 174:120–130. https://doi.org/10.1016/j.marchem.2015.05.005

Lannuzel D, Vancoppenolle M, van der Merwe P, et al (2016) Iron in sea ice: Review and new insights. Elementa: Science of the Anthropocene. 4: 000130. DOI: https://doi.org/10.12952/journal.elementa.000130

Lieser JL, Curran MAJ, Bowie AR et al (2015) Antarctic slush-ice algal accumulation not quantified through conventional satellite imagery: beware the ice of March. Cryosphere Discussions 9:6187–6222. https://doi.org/10.5194/tcd-9-6187-2015

Lin H, Rauschenberg S, Hexel CR et al (2011) Free-drifting icebergs as sources of iron to the Weddell Sea. Deep Sea Res Part II 58:1392–1406. https://doi.org/10.1016/j.dsr2.2010.11.020

Lis H, Shaked Y, Kranzler C et al (2015) Iron bioavailability to phytoplankton: an empirical approach. ISME J 9:1003–1013. https://doi.org/10.1038/ismej.2014.199

Lizotte MP (2003) The Microbiology of sea ice. In: Thomas DN, Dieckmann GS (eds) sea ice. Blackwell Science Ltd, Oxford. https://doi.org/10.1002/9780470757161.ch6

Maldonado MT, Price NM (1996) Influence of N substrate on Fe requirements of marine centric diatoms. Mar Ecol Prog Ser 141:161–172

Maldonado MT, Price NM (1999) Utilization of iron bound to strong organic ligands by plankton communities in the subarctic Pacific Ocean. Deep Sea Res Part II 46:2447–2473. https://doi.org/10.1016/S0967-0645(99)00071-5

Marchetti A, Parker MS, Moccia LP et al (2009) Ferritin is used for iron storage in bloom-forming marine pennate diatoms. Nature 457:467–470. https://doi.org/10.1038/nature07539

McKay RML, Wilhelm SW, Hall J et al (2005) Impact of phytoplankton on the biogeochemical cycling of iron in subantarctic waters southeast of New Zealand during FeCycle. Global Biogeochem Cycles 19:GB4S24. https://doi.org/10.1029/2005GB002482

Menden-Deuer S, Lessard EJ (2000) Carbon to volume relationships for dinoflagellates, diatoms, and other protist plankton. Limnol Oceanogr 45:569–579

Miller LA, Fripiat F, Else BGT et al (2015) Methods for biogeochemical studies of sea ice: the state of the art, caveats, and recommendations. Elementa: Sci Anthropocene 3:000038. https://doi.org/10.12952/journal.elementa.000038

Mock T (2002) In situ primary production in young Antarctic sea ice. Hydrobiologia 470:127–132

Moore C, Mills M, Arrigo K et al (2013) nutrient limitation. Nat Geosci 6:701–710. https://doi.org/10.1038/NGEO1765

Morán XAG, Gasol JM, Arin L et al (1999) A comparison between glass fiber and membrane filters for the estimation of phytoplankton POC and DOC production. Mar Ecol Prog Ser 187:31–41. https://doi.org/10.3354/meps187031

Moreau S, Lannuzel D, Janssens J et al (2019) Sea-ice meltwater and circumpolar deep water drive contrasting productivity in three Antarctic polynyas. J Geophys Res: Oceans 124:2943–2968. https://doi.org/10.1029/2019JC015071

Nicolaus M, Haas C, Willmes S (2009) Evolution of first-year and second-year snow properties on sea ice in the Weddell Sea during spring-summer transition. J Geophys Res: Atmosphere 114:D17109. https://doi.org/10.1029/2008JD011227

Person R, Vancoppenolle M, Aumont O (2020) Iron incorporation from seawater into Antarctic sea ice: a model study. Global Biogeochem Cycles 34:e2020GB006665. https://doi.org/10.1029/2020GB006665

Planquette H, Statham PJ, Fones GR et al (2007) Dissolved iron in the vicinity of the Crozet Islands, Southern Ocean. Deep Sea Res Part II 54:1999–2019. https://doi.org/10.1016/j.dsr2.2007.06.019

Planquette H, Sanders RR, Statham PJ et al (2011) Fluxes of particulate iron from the upper ocean around the Crozet Islands: a naturally iron-fertilized environment in the Southern Ocean. Global Biogeochem Cycles 25:GB2011. https://doi.org/10.1029/2010GB003789

Pollard RT, Salter I, Sanders RJ et al (2009) Southern Ocean deep-water carbon export enhanced by natural iron fertilization. Nature 457:577–580. https://doi.org/10.1038/nature07716

Porter KG, Feig YS (1980) The use of DAPI for identifying and counting aquatic microflora. Limnol Oceanogr 25:943–948

Raiswell R, Tranter M, Benning LG et al (2006) Contributions from glacially derived sediment to the global iron (oxyhydr)oxide cycle: Implications for iron delivery to the oceans. Geochim Cosmochim Acta 70:2765–2780. https://doi.org/10.1016/j.gca.2005.12.027

Raiswell R, Benning LG, Tranter M et al (2008) Bioavailable iron in the Southern Ocean: the significance of the iceberg conveyor belt. Geochem Trans 9:1–9. https://doi.org/10.1186/1467-4866-9-7

Raven JA, Geider RJ (1988) Temperature and algal growth. New Phytol 110:441–461. https://doi.org/10.1111/j.1469-8137.1988.tb00282.x

Raymond B, Meiners K, Fowler CW et al (2009) Cumulative solar irradiance and potential large-scale sea-ice algae distribution off East Antarctica (30°E–150°E). Polar Biol 32:443–452. https://doi.org/10.1007/s00300-008-0538-5

Rintala J-M, Piiparinen J, Blomster J et al (2014) Fast direct melting of brackish sea-ice samples results in biologically more accurate results than slow buffered melting. Polar Biol 37:1811–1822. https://doi.org/10.1007/s00300-014-1563-1

Rose JM, Feng Y, Ditullio GR et al (2009) Synergistic effects of iron and temperature on Antarctic phytoplankton and microzooplankton assemblages. Biogeosciences 6:3131–3147. https://doi.org/10.5194/bg-6-3131-2009

Roukaerts A, Cavagna A-J, Fripiat F et al (2015) Sea-ice algal primary production and nitrogen uptake rates off East Antarctica. Deep Sea Res Part II: Topical Stud Oceanogr. https://doi.org/10.1016/j.dsr2.2015.08.007

Sarthou G, Timmermans KR, Blain S et al (2005) Growth physiology and fate of diatoms in the ocean: a review. J Sea Res 53:25–42. https://doi.org/10.1016/j.seares.2004.01.007

Sarthou G, Vincent D, Christaki U et al (2008) The fate of biogenic iron during a phytoplankton bloom induced by natural fertilisation: impact of copepod grazing. Deep-Sea Research Part II: Topical Studies in Oceanography 55:734–751. https://doi.org/10.1016/j.dsr2.2007.12.033

Schoemann V, Wollast R, Chou L et al (2001) Effects of photosynthesis on the accumulation of Mn and Fe by Phaeocystis colonies. Limnol Oceanogr 46:1065–1076. https://doi.org/10.4319/lo.2001.46.5.1065

Sedwick PN, DiTullio GR (1997) Regulation of algal blooms by the release of iron from in Antarctic shelf melting sea ice. Geophys Res Lett 24:2515–2518

Shaw TJ, Raiswell R, Hexel CR et al (2011) Input, composition, and potential impact of terrigenous material from free-drifting icebergs in the Weddell Sea. Deep Sea Res Part II 58:1376–1383. https://doi.org/10.1016/j.dsr2.2010.11.012

Smith WO Jr, Nelson DM (1985) Phytoplankton Bloom Produced by a receding ice edge in the Ross Sea: spatial coherence with the density field. Science 227:163–166

St-Laurent P, Yager PL, Sherrell RM et al (2019) Modeling the seasonal cycle of iron and carbon fluxes in the Amundsen Sea Polynya, Antarctica. J Geophys Res: Oceans. https://doi.org/10.1029/2018JC014773

Strzepek RF, Maldonado MT, Higgins JL et al (2005) Spinning the "Ferrous Wheel": the importance of the microbial community in an iron budget during the FeCycle experiment. Global Biogeochem Cycles 19:GB4S26. https://doi.org/10.1029/2005GB002490

Strzepek RF, Maldonado MT, Hunter KA et al (2011) Adaptive strategies by Southern Ocean phytoplankton to lessen iron limitation: uptake of organically complexed iron and reduced cellular iron requirements. Limnol Oceanogr 56:1983–2002. https://doi.org/10.4319/lo.2011.56.6.1983

Sunda W, Huntsman S (1995) Iron uptake and growth limitation in oceanic and coastal phytoplankton. Mar Chem 50:189–206

Sunda WG, Huntsman SA (1997) Interrelated influence of iron, light and cell size on marine phytoplankton growth. Nature 390:389–392

Sunda WG, Huntsman SA (2011) Interactive effects of light and temperature on iron limitation in a diatom: implications for marine productivity and carbon cycling. Limnol Oceanogr 56:1475–1488. https://doi.org/10.4319/Lo.2011.56.4.1475

Tang D, Morel FMM (2006) Distinguishing between cellular and Fe-oxide-associated trace elements in phytoplankton. Mar Chem 98(1):18–30. https://doi.org/10.1016/j.marchem.2005.06.003

Taylor RL, Semeniuk DM, Payne CD et al (2013) Colimitation by light, nitrate, and iron in the Beaufort Sea in late summer. Journal of Geophysical Res: Oceans 118:3260–3277

Thomas DN, Dieckmann GS (2002) Biogeochemistry of Antarctic sea ice. Oceanogr Marine Biol 40:143–169

Timmermans KR, van der Wagt B, de Baar HJW (2004) Growth rates, half saturation constants, and silicate, nitrate, and phosphate depletion in relation to iron availability of four large open-ocean diatoms from the Southern Ocean. Limnol Oceanogr 49:2141–2151. https://doi.org/10.4319/lo.2004.49.6.2141

Tison J-L, Worby A, Delille B et al (2008) Temporal evolution of decaying summer first-year sea ice in the Western Weddell Sea, Antarctica. Deep Sea Res Part II 55:975–987. https://doi.org/10.1016/j.dsr2.2007.12.021

Tortell PD, Maldonado MT, Price NM (1996) The role of heterotrophic bacteria in iron-limited ocean ecosystems. Nature 383:330–332. https://doi.org/10.1038/383330a0

Tortell PD, Mills MM, Payne CD et al (2013) Inorganic C utilization and C isotope fractionation by pelagic and sea-ice algal assemblages along the Antarctic continental shelf. Mar Ecol Prog Ser 483:47–66. https://doi.org/10.3354/meps10279

Tovar-Sanchez A, Sañudo-Wilhelmy SA, Garcia-Vargas M et al (2003) A trace metal clean reagent to remove surface-bound iron from marine phytoplankton. Mar Chem 82:91–99. https://doi.org/10.1016/S0304-4203(03)00054-9

Twining BS, Baines SB, Fisher NS et al (2004) Cellular iron contents of plankton during the Southern Ocean iron experiment (SOFeX). Deep Sea Res Part I 51:1827–1850. https://doi.org/10.1016/j.dsr.2004.08.007

Twining BS, Baines SB (2013) The trace metal composition of marine phytoplankton. Ann Rev Mar Sci 5:191–215. https://doi.org/10.1146/annurev-marine-121211-172322

Twining BS, Antipova O, Chappell PD et al (2021) Taxonomic and nutrient controls on phytoplankton iron quotas in the ocean. Limnol Oceanogr Lett 6:96–106. https://doi.org/10.1002/lol2.10179

Underwood GJC, Fietz S, Papadimitriou S et al (2010) Distribution and composition of dissolved extracellular polymeric substances (EPS) in Antarctic sea ice. Mar Ecol Prog Ser 404:1–19

Utermölh H (1958) Zur Vervelkommnung der quantitativen Phytoplankton- Methodik. Mitt Int Verein Theor Angew Limnol 9:1–38

van der Merwe P, Lannuzel D, Mancuso Nichols CA et al (2009) Biogeochemical observations during the winter–spring transition in East Antarctic sea ice: evidence of iron and exopolysaccharide controls. Mar Chem 115(3–4):163–175. https://doi.org/10.1016/j.marchem.2009.08.001

van der Merwe P, Wuttig K, Holmes T et al (2019) High lability Fe particles sourced from glacial erosion can meet previously unaccounted biological demand: Heard Island, Southern Ocean. Front Mar Sci 6:1–20. https://doi.org/10.3389/fmars.2019.00332

Veldhuis MJW, Timmermans KR, Croot P et al (2005) Picophytoplankton: a comparative study of their biochemical composition and photosynthetic properties. J Sea Res 53:7–24. https://doi.org/10.1016/j.seares.2004.01.006

Verdugo P, Alldredge AL, Azam F et al (2004) The oceanic gel phase: a bridge in the DOM-POM continuum. Marine Chem 92:67–85

Wang S, Bailey D, Lindsay K et al (2014) Impact of sea-ice on the marine iron cycle and phytoplankton productivity. Biogeosciences 11:4713–4731. https://doi.org/10.5194/bg-11-4713-2014

Welschmeyer NA, Lorenzen CJ (1984) Carbon- 14 labeling of phytoplankton carbon and chlorophyll a carbon: determination of specific growth rates'. Limnol Oceanogr 29(1):135–145

Yentsch CS, Menzel DW (1963) A method for the determination of phytoplankton chlorophyll and phaeophytin by fluorescence. Deep-Sea Res Oceanogr Abstr 10(3):221–231

Yager PL, Deming JW (1999) Pelagic microbial activity in an arctic polynya: testing for temperature and substrate interactions using a kinetic approach. Limnol Oceanogr 44:1882–1893